http://dx.doi.org/10.5012/bkcs.2012.33.5.1722

Theoretical Explanation of the Peak Splitting of Tobacco-Specific *N*-Nitrosamines in HPLC

Juxing Jiang,[†] Liangchun Li,[‡,*] Mingfeng Wang,[†] Jianjun Xia,[†,§] Wenyuan Wang,[†] and Xiaoguang Xie[§]

[†]*Technology Center, Hongyun-Honghe Tobacco (Group) Co., Ltd., Kunming 650202, China*
[‡]*Key Laboratory of Drug-Targeting of Education Ministry and Department of Medicinal Chemistry, West China School of Pharmacy, Sichuan University, Chengdu 610041, China. *E-mail: lilc76@gmail.com*
[§]*Department of Chemistry, Yunnan University, Kunming 650091, China*
Received November 30, 2011, Accepted February 23, 2012

During the analyzing processes of the compounds, some researchers are puzzled by the analytical signals for some TSNAs (with or without splitting peaks at various pHs and temperatures). In this work, a detailed theoretical study of structural and thermal properties of the *E*/*Z* isomers of TSNAs and the corresponding protonated structures was performed using DFT methods. The calculations showed that the *E* isomers are almost stable than *Z* isomers, while the *Z* isomers would be more stable when in protonation. The calculated results predicted the possibility of separation of their *E* and *Z* isomer forms and also showed that protonation affects the dipole moment of molecules significantly (0.1-0.5 to 0.7-2.1 Debye). The calculations agreed well with the experiments that the split-up of the HPLC signal for TSNAs into two peaks are very sensitive to the pH and temperature of the mobile-phase.

Key Words : TSNAs, E/Z isomers, Protonation, Peak-splitting

Introduction

Tobacco-specific *N*-nitrosamines (TSNAs) are a group of powerful pulmonary carcinogens found in tobacco products, mainly including *N*-nitrosonornicotine (NNN), (4-methylnitrosoamino)-1-(3-pyridyl)-1-butanone (NNK), *N*-nitrosoanabasine (NAB) and N-nitrosoanatabine (NAT). The mechanism of their toxicity involves metabolic reactions of nitrosamines with cytochrome P-450 enzyme. For their importance of cancer researches, TSNAs have attracted great interests in recent years.[1] In most cases, these research papers focus on the determination of TSNAs in tobacco smoke or their metabolites in urine. Up to now a number of analytical techniques have been employed for measuring these compounds. Two most widely used methods[2-5] are gas chromatography coupled with a thermal energy analyzer (GC-TEA)[1] and liquid chromatography coupled to tandem mass spectrometry (LC-MS/MS).[6] Recently, methods of gas chromatography coupled to ion-trap tandem mass (GC-ITMS),[7] capillary electrophoresis-electrospray ionization mass spectrometry (CE-MS),[8] and micellar electrokinetic chromatography (MEKC) method combined with cation selective exhaustive injection (CSEI) and sweeping (CSEI-Sweep-MEKC)[3] are also used to quantitate the four TSNAs and even their metabolites.

In these papers, the analytical methods vary from each other, but some researchers are confronted with the case that the analytical signals for some TSNAs are splitting into double-peaks. Literally, all the peaks of NNN,[8,9] NAT,[9] NNK,[3,8,10] and NNAL[3,10,11] can split into two peaks in certain conditions. In achiral separation condition, the peak-splitting is generally believed to be due to the co-existence of *E*/*Z* isomers rather than their enantiomers. But some researchers are puzzled by the causes of the phenomenon every now and then. For example, McCorquodale *et al.* observed that the baseline between peaks assigned to (*R*)-NNN and (*S*)-NNN did not return to its original position and presumed that there was an enantiomeric interconversion.[12] Li and Jansson *et al.* considered that the split-up of the signal was probably due to the basicity of TSNAs and the formation of their protonated isomers.[8] Hecht *et al.* reported that nitrosamines existed as mixture of *E* and *Z* isomers.[13] Wu *et al.* found that all TSNAs could exhibit some degree of shoulder effects or split peaks. Dissolving standards into different pH buffer solutions for LC/MS/MS analysis, they obtained different split peak ratios, which suggested that one isomer could be favored over another under certain pH condition. With careful column selection and optimization, they achieved good peak shapes without splitting at pH = 5.[14] Apparently, this behavior of TSNAs is pH dependent. According to our statistics, signals for TSNAs tend to split up in acid analytical condition at room temperature. But no such phenomenon is observed when the column temperature is at 60 ºC or when ammonium acetate is used only to adjust the pH of the mobile phase. Thus, the signals for TSNAs splitting into double-peaks can be attributed to the pH and temperature of the mobile phase of the analytical procedures.

In these TSNAs, the N-NO single bond has a partial double bond character due to the $n_N \rightarrow \pi_{NO}$ conjugate (Scheme 1), which leads to the nature that the rotation of the N-NO bond is somewhat restricted. The restricted rotation around the N-NO bond in nitrosamine compounds has attracted several experimental and theoretical investigations for years.[15-20] These authors studied the isomer populations and rotational

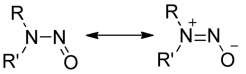

Scheme 1. Main resonance hybrids of TSNAs.

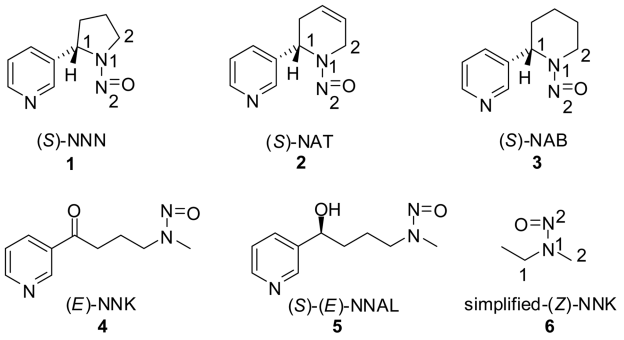

Figure 1. Chemical structures of the TSNAs.

barriers in simple H_2NNO and some of cyclic nitrosamine compounds by dynamic NMR techniques[20] and *Ab initio* methods. These studies pointed out that a) the determination of activation barriers to N-N rotation provide quantitative information about the N-NO π-dative bonding;[19] b) substitution of the hydrogen atoms of H_2NNO molecule by methyl groups or other alkyl groups leads to a stronger NN double bond (by at least 3 kcal/mol).[18] In this paper, we report the theoretical calculations of the TSNAs' and their protonations' structural, energetic and charge population properties in gas phase in order to understand the interconversion mechanisms of their *E-Z* isomers and to elucidate the reasons of peak-splitting.

Among these *N*-nitrosamines, there is a chiral center for NNN, NAT and NAB (Figure 1), respectively, and actually *S* enantiomers are in majority in tobacco products.[5,21] In this study, properties of *S* enantiomers of TSNAs are mainly calculated and a simplified model structure **6** was calculated for NNK and NNAL.

Computational Method

The geometrical structures and energetic properties for each *E* and *Z* isomers of NNN, NAT, NAB, simplified-NNK and their transition states of isomerization have been calculated with GAUSSIAN 03 package.[22] The structures of all isomers of the four TSNAs are fully scanned at HF/sto-3G level. All local minimum energy conformations are reoptimized at B3LYP/6-31G* level to obtain global minima.[23,24] The minimum energy structures have been further performed at B3LYP and M05[25] levels with the 6-311++G(2d,2p) and 6-311++G(d,p) basis sets for more accurate geometric structures. Vibrational analysis is performed for all stationary structures to confirm their stability and also to provide the frequencies needed for the calculation of the relative Gibbs free energies (ΔG). The transition states are confirmed to have only a single imaginary frequency. Intrinsic reaction coordinate (IRC) calculations are performed in order to verify that the localized transition state structures connect with the corresponding minimum points (the *E* and *Z* isomers). NBO charges have also been obtained, through a NBO populational analysis.[26] These charges have been considered as a more "realistic" alternative to Mulliken charges.[27] In what follows, the discussed energies are relative Gibbs free energies (ΔG_{298K}). The relative electronic energies (ΔE) and enthalpies (ΔH_{298K}) are also provided for reference.

For the isomerization of E to Z forms, their equilibrium constants (K_{eq}) are calculated as shown by the following relations:

$$\ln k = \frac{\Delta G}{RT}, \tag{1}$$

where ΔG is the relative Gibbs free energy, R is the gas constant and T is the temperature (K).

Proton affinity (PA), which is defined as the enthalpy change during the protonation process in gas-phase at 298 K, is calculated using the equation:

$$PA = \Delta H\,(TSNA) + \Delta H\,(H^+) - \Delta H\,(TSNA\text{-}H^+), \tag{2}$$

where $\Delta H\,(H^+) = 2.5\,RT = 1.48$ kcal/mol.[28]

Results and Discussion

Although there are a few literatures revealed that even the high-level *Ab initio* (MP2 and CCSD)[18] methods cannot give the accurate results for H_2NNO, DFT methods give a balance between the *accuracy* and computational *cost* for more complex substituted *N*-nitrosamine compounds. We optimized the final structures by choosing B3LYP with 6-311++G(2d,2p) and 6-311++G(d,p) basis sets in our researches. For comparison, M05/6-311++G(d,p) was also applied for calculation because M05 is reported that it is *good* for calculation of the bond dissociation energies.

The optimized structural parameters of the *E/Z* isomers and their transition states (TS) of **1**, **2**, **3** and **6** in gas phase are partially listed in Table 1-4, respectively. The N-N bond lengths in the *E*/*Z* isomers are in the range of 1.318-1.336 Å and the values are almost the same as the results calculated by different methods. As shown in these tables, N=O and N-C bond lengths are in the range of 1.21-1.23 Å and 1.45-1.48 Å, respectively, which calculated by B3LYP methods are greater than M05 calculated results by at most 0.019 Å. Comparing with the normal N-N single bond length (~1.45 Å) and N=O double bond length (~1.18 Å), these results clearly show that the N-N single-bond length and the N=O double-bond length are in the trend of equalization due to the $n_N \rightarrow \pi_{NO}$ conjugation effect in the molecules. The calculated bond angles of the four *E* isomers of TSNAs are in the ranges from 116.4 to 124.7° (<CNN), from 114.8 to 116.5° (<NNO), and from 114.0 to 122.6° (<CNC), while the corresponding angles of Z isomers are in the ranges from 116.4 to 123.8°, from 115.0 to 116.6°, and from 113.3 to 121.3°, respectively. The calculated dihedral angles (<CNNO) of the *E* and *Z* isomers of four TSNAs are in the ranges from 174.6 to 178.1° and from −0.5 to 12.0°, respectively. The planarity of the C_2NNO atoms in *N*-nitrosodimethylamine is

Table 1. Calculated optimized geometric structural parameters for *E*, *Z* isomer forms and TS of compound **1** at B3LYP/6-311++G(d,p) (Basis set I), B3LYP/6-311++G(2d,2p) (Basis set II) and M05/6-311++G(d,p) (Basis set III) levels, respectively

Compounds	(*S*)-*E*-**1**			(*S*)-*Z*-**1**			TS		
Basis set	I	II	III	I	II	III	I	II	III
Bond length (Å)									
N1-N2	1.320	1.318	1.319	1.327	1.326	1.325	1.504	1.504	1.496
N2-O	1.227	1.228	1.214	1.224	1.225	1.211	1.177	1.177	1.168
N1-C1	1.478	1.476	1.468	1.483	1.480	1.472	1.487	1.487	1.474
N1-C2	1.473	1.470	1.463	1.468	1.466	1.457	1.481	1.480	1.469
Bond angle (°)									
C1-N1-N2	120.454	120.468	120.412	123.159	122.885	123.352	106.322	106.056	106.333
N1-N2-O	114.831	114.868	115.053	114.989	115.027	115.085	112.576	112.608	112.605
C1-N1-C2	114.237	114.215	113.979	113.504	113.404	113.270	104.130	104.011	103.866
C2-N1-N2	124.371	124.296	124.679	119.534	119.263	119.960	105.887	105.621	105.927
Dihedral angle (°)									
C1-N1-N2-O	-175.012	-174.632	-175.094	10.962	12.021	10.489	124.076	124.162	125.042

Table 2. Calculated optimized geometric structural parameters for *E*, *Z* isomer forms and TS of compound **2** at B3LYP/6-311++G(d,p) (Basis set I), B3LYP/6-311++G(2d,2p) (Basis set II) and M05/6-311++G(d,p) (Basis set III) levels, respectively

Compounds	(*S*)-*E*-**2**			(*S*)-*Z*-**2**			TS		
Basis set	I	II	III	I	II	III	I	II	III
Bond length (Å)									
N1-N2	1.332	1.330	1.331	1.331	1.329	1.330	1.539	1.539	1.533
N2-O	1.222	1.224	1.210	1.223	1.224	1.210	1.178	1.178	1.168
N1-C1	1.468	1.466	1.460	1.478	1.475	1.469	1.482	1.480	1.471
N1-C2	1.462	1.459	1.453	1.458	1.455	1.450	1.475	1.474	1.464
Bond angle (°)									
C1-N1-N2	116.708	116.742	116.903	123.805	123.763	123.836	109.637	109.451	109.719
N1-N2-O	115.913	115.969	116.006	116.543	116.611	116.556	113.566	113.643	113.652
C1-N1-C2	120.366	120.473	120.099	119.374	119.412	119.155	112.081	111.895	112.075
C2-N1-N2	122.833	122.736	122.954	116.777	116.738	116.958	107.236	107.072	107.296
Dihedral angle (°)									
C1-N1-N2-O	176.185	176.572	177.099	3.422	3.798	3.531	-61.075	-60.994	-61.315

Table 3. Calculated optimized geometric structural parameters for *E*, *Z* isomer forms and TS of compound **3** at B3LYP/6-311++G(d,p) (Basis set I), B3LYP/6-311++G(2d,2p) (Basis set II) and M05/6-311++G(d,p) (Basis set III) levels, respectively

Compounds	(*S*)-*E*-**3**			(*S*)-*Z*-**3**			TS		
Basis set	I	II	III	I	II	III	I	II	III
Bond length (Å)									
N1-N2	1.336	1.333	1.334	1.332	1.330	1.330	1.536	1.536	1.529
N2-O	1.221	1.223	1.209	1.223	1.225	1.211	1.179	1.179	1.169
N1-C1	1.467	1.464	1.459	1.478	1.475	1.470	1.480	1.479	1.470
N1-C2	1.467	1.463	1.458	1.461	1.458	1.453	1.477	1.475	1.466
Bond angle (°)									
C1-N1-N2	116.447	116.444	116.598	123.637	123.540	123.589	109.221	109.058	109.328
N1-N2-O	116.468	116.543	116.454	116.534	116.587	116.551	113.575	113.659	113.696
C1-N1-C2	119.279	119.387	119.160	119.182	119.323	119.094	112.460	112.276	112.477
C2-N1-N2	124.075	123.976	124.028	116.937	116.865	117.039	107.462	107.287	107.586
Dihedral angle (°)									
C1-N1-N2-O	-177.785	-177.932	-177.649	4.371	4.699	4.561	-62.175	-62.056	-62.483

observed in both the crystalline solid state[29] and the gas-phase structures, which is consistent with the NMR results.[18] According to our calculated simplified structure **6**, the calculated values for the CNNO dihedral angle are very close to planar (by at most 3.2° with M05 method). However, there were no experimental values about these TSNAs, we

Table 4. Calculated optimized geometric structural parameters for *E*, *Z* isomer forms and TS of simplified model compound **6** at B3LYP/6-311++G(d,p) (Basis set I), B3LYP/6-311++G(2d,2p) (Basis set II) and M05/6-311++G(d,p) (Basis set III) levels, respectively

Compounds	(*S*)-*E*-**6**			(*S*)-*Z*-**6**			TS		
Basis set	I	II	III	I	II	III	I	II	III
Bond length (Å)									
N1-N2	1.328	1.325	1.330	1.332	1.330	1.332	1.509	1.509	1.500
N2-O	1.225	1.226	1.210	1.223	1.225	1.210	1.178	1.178	1.169
N1-C1	1.460	1.457	1.452	1.465	1.462	1.456	1.481	1.480	1.471
N1-C2	1.459	1.456	1.449	1.452	1.449	1.443	1.468	1.467	1.457
Bond angle (°)									
C1-N1-N2	116.716	116.783	116.459	122.293	122.236	122.431	106.620	106.451	106.752
N1-N2-O	115.075	115.073	115.675	115.672	115.722	115.891	111.715	111.725	111.751
C1-N1-C2	122.491	122.569	121.955	121.302	121.342	121.198	113.596	113.414	113.933
C2-N1-N2	120.753	120.631	121.519	116.392	116.416	116.365	105.435	105.149	105.524
Dihedral angle (°)									
C1-N1-N2-O	177.596	178.065	176.813	-0.476	-0.836	-0.642	-119.615	-119.797	-119.293

can only compare the values with the analogous structures such as some monocyclic aliphatic *N*-nitrosamines and the agreement between our results and the experimental results is generally good. For example, some of the measured geometry parameters were: N-N bond lengths from 1.29 to 1.31 Å, the N-O bond lengths from 1.23 to 1.25 Å and NNO angles from 112.7 to 114.7°.[30] Thus, our calculated methods are very well to describe these TSNAs structures and the M05 method can better describe the N-N bond length than B3LYP.

The potential scan for the internal rotation about the N-N bond showed that the rotation in the *N*-nitrosamines may follow two pathways. Thus, there are two possible transition states for internal rotation between the two isomers. The possible TSs taking NNN for examples are shown and labeled in Scheme 2. After comparing the calculated results using different basis sets, one dominant transition state structure was always provided. The structural characteristics in TSs show some difference: a) larger N-N bond length (from 1.500 to 1.539 Å) and shorter N-O bond length (from 1.168 to 1.179 Å) than in the ground state; b) smaller <NNO bond angle than in ground state; c) the M05 calculated structures show slight shorter N-N, N-O bond length and bigger <NNO bond angle than B3LYP.

Roohi's calculation results[16] show that chair conformations are the most stable conformations for both *E* and *Z* isomers for six-membered cyclic nitrosamine compounds. Our calculations of the relative Gibbs free energies (ΔG) also confirm this result. But it is out of expectation that the pyridyl group of (*S*)-NAB in axial position is more stable than that in equatorial position.

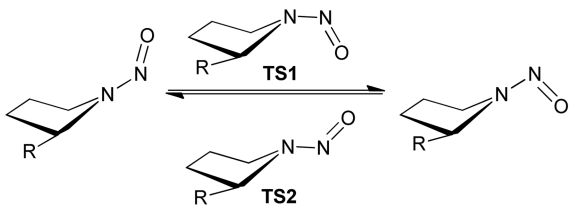

Scheme 2. The possible TSs of the internal rotation of NNN.

The relative Gibbs free energies (ΔG_{298K}) of the *E* and *Z* isomers of **1**, **2**, **3** and **6**, calculated using B3LYP and M05 methods are listed in Table 5. For **1**, **2** and **6**, the *E* isomers are more stable than the *Z* isomers by 3.31, 1.61 and 2.94 kJ/mol at B3LYP/6-311++G(2d,2p) level, and 7.58, 0.75, 2.08 kJ/mol at M05/6-311++G(d,p) level, respectively. For S-NAB (**3**) the calculated results show that *Z* isomer is stable (by 0.54 kJ/mol) at B3LYP/6-311++G(2d,2p) level, while the calculated results using M05 shows *E* isomer is stable (by 0.67 kJ/mol). As shown in table 5, the relative internal rotation activation Gibbs free energy (ΔG_{298K}) in the **1**, **2**, **3** and **6** are as follows: 90.98, 103.26, 96.32 and 111.78 kJ/mol at B3LYP/6-311++G(2d,2p) level; 92.21, 110.81, 105.59 and 118.29 kJ/mol at M05/6-311++G(d,p) level, respectively. These results show that the calculated rotational ΔG_{298K} barriers at M05 level are larger than those at B3LYP level. Considering M05 is especially *good* for calculation of the bond dissociation energies, we calculated the equilibrium constants (K_{eq}), Boltzmann populations (*P*) for the isomerization of *E* to *Z* forms and dipole moment (μ) by using M05/6-311++G(d,p) method.

An isomeric form of a molecule can be separated at room temperature if the activation barrier energy for interconversion is at least 80 kJ/mol.[15] The calculated barrier energies for interconversion of the isomers in the TSNAs are greater than 80 kJ/mol, therefore, the calculated results can predict the possibility of separation of their *E* and *Z* isomer forms. Although the solvent effects are not considered in this moment due to the greater computational cost, the calculated dipole moments show some clues. As shown in Table 5, the calculated dipole moment of TSs for **1** and **6** show lower values than those of ground states, which mean the energy barriers would increase in polar solvents. It is interesting that the calculated dipole moment of TS for *S*-NAT (**2**) and S-NAB (**3**) show opposite value, which suggests that *S*-NAT (**2**) and S-NAB (**3**) in polar solvent (like methanol) would be hard to see peak-splitting in HPLC analysis at room temperature.[9] Additionally, according to the calculated K_{eq} (>1),

Table 5. Calculated relative electronic energies (ΔE), Gibbs free energy (ΔG_{298K}), enthalpy (ΔH_{298K}), equilibrium constants (K_{eq}), Boltzmann populations (P) for the isomerization of E to Z forms and dipole moment (μ) at B3LYP/6-311++G(d,p) (Basis set I), B3LYP/6-311++G(2d,2p) (Basis set II) and M05/6-311++G(d,p) (Basis set III) levels, respectively

Species	ΔE (kJ/mol)			ΔG_{298K} (kJ/mol)			ΔH_{298K} (kJ/mol)			K_{eq}	P (%)	μ (debye)
Basis sets	I	II	III	I	II	III	I	II	III	III	III	III
1-E	0.0	0.0	0.0	0.0	0.0	0.0	0.0	0.0	0.0	21.32	95	4.78
1-Z	2.11	1.67	1.71	3.64	3.31	7.58	2.34	1.91	-0.55		5	4.84
1-TS	96.48	94.77	101.39	92.43	90.98	92.21	91.40	89.70	96.06			4.12
2-E	0.0	0.0	0.0	0.0	0.0	0.0	0.0	0.0	0.0	1.35	57	2.09
2-Z	1.11	1.12	0.11	1.34	1.61	0.75	1.36	1.40	0.63		43	1.90
2-TS	109.61	107.18	115.18	105.39	103.26	110.81	102.76	100.43	108.58			2.81
3-E	0.0	0.0	0.0	0.0	0.0	0.0	0.0	0.0	0.0	1.31	56	2.27
3-Z	-1.46	-1.52	-2.23	-0.52	-0.54	0.67	-1.40	-1.48	-1.96		44	2.72
3-TS	103.60	101.29	109.41	98.60	96.32	105.59	96.61	94.34	103.08			3.31
6-E	0.0	0.0	0.0	0.0	0.0	0.0	0.0	0.0	0.0	2.31	69	4.44
6-Z	1.53	1.36	0.65	2.52	2.94	2.08	1.75	1.61	0.68		31	4.25
6-TS	115.06	114.01	119.79	112.78	111.78	118.29	108.85	107.75	113.77			2.34

which are listed in Table 5, one dominant isomer of TSNAs are expected to be significantly populated at certain higher temperature. Thus, some HPLC experiments showed peak-splitting at room temperature, while no such phenomenon is observed when the column temperature is at 60 ºC, which are consistent with our calculations very well.

The ratios of the calculated Boltzmann populations of the *E* and *Z* isomers of TSNAs coincide well with the reported chromatograms, which *E* isomers are mainly favored than *Z* isomers in TSNAs.[3,8-11] But it should be noted that all of those chromatogram results are obtained in acidic condition or with acidic mobile phase. Through the procedure of sample preparation for the determination of TSNAs' metabolites in urine, it is shown that TSNAs exist as cations in acidic condition and as free states at pH of 9-10.[4] Hence, the energetic and structural parameters for pronated TSNAs should also be calculated in comparison with those for free TSNAs.

There are one oxygen and three nitrogen atoms in every TSNAs' molecule. Each atom in molecule has the possibility to accept a proton and form different protonated structures in acidic condition. To find which atom in the molecule is most possible to accept a proton, it is necessary to perform the natural bond orbital (NBO) analysis for TSNAs. Then, structural and thermal properties of their protonated forms can be calculated.

Natural bond orbital (NBO) analysis is performed with the optimized structures of *S*-NNN, *S*-NAT, *S*-NAB and simplified-NNK to obtain reliable atomic charges. The NBO charges of the atoms of the TSNAs are listed in Table 6. Obviously, the NBO charges on the corresponding three atoms in N-NO group of the TSNAs including simplified-NNK are very close. The NBO charges on the N atoms of pyridyl of (*S*)-(*E*)-NNN, (*S*)-(*E*)-NAT and (*S*)-(*E*)-NAB are almost identical. In generally, the N atoms of pyridyl of the TSNAs are the most negative of all the atoms of N and O in these molecules. This fact indicates that the N atom of pyridyl of the TSNAs is the most likely atom to accept a proton in the molecules.

We have further calculated three most possible conformers of protonated *E* and *Z* isomers of (*S*)-NNN respectively at M05/6-311++G(d,p) level. The proton affinity (PA) values of E and Z isomers of three most possible protonation sites for (S)-NNN (illustrated by Figure 2) are listed in Table 7. The results are perfectly in accord with the results of NBO charges and the protonation site of the TSNAs is the nitrogen atom of pyridyl. Due to the weak acidic condition in experiment, the possibility of the diprotonated structures of TSNAs should be very small and it was not considered in this investigation.

The optimized geometric structures of these protonated TSNAs show little changes from non-protonated structures. The calculated thermal parameters of the protonated TSNAs,

Table 6. NBO charges of the *E* and *Z* isomers of the TSNAs at the M05\6-311++G(d,p)\\ M05\6-311++G(d,p) level

Species	(*S*)-*E*-**1**	(*S*)-*Z*-**1**	TS-**1**	(*S*)-*E*-**2**	(*S*)-*Z*-**2**	TS-**2**	(*S*)-*E*-**3**	(*S*)-*Z*-**3**	TS-**3**	*E*-**6**	*Z*-**6**	TS-**6**
N1	-0.292	-0.293	-0.474	-0.243	-0.280	-0.479	-0.294	-0.290	-0.489	-0.283	-0.286	-0.469
N2	0.218	0.221	0.285	0.215	0.223	0.325	0.212	0.218	0.324	0.208	0.209	0.275
O=N	-0.414	-0.406	-0.215	-0.412	-0.417	-0.232	-0.411	-0.417	-0.235	-0.418	-0.419	-0.222
N of Py	-0.458	-0.459	-0.460	-0.461	-0.461	-0.461	-0.460	-0.460	-0.462	-[a]	-[a]	-[a]

[a]not calculated.

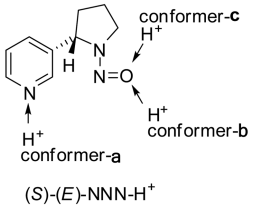

Figure 2. Three most possible protonation sites of (*S*)-(*E*)-NNN.

namely protons adding to the nitrogen atom of pyridyl in TSNAs, are listed in Table 8. For (*S*)-NNN and (*S*)-NAT, the relative Gibbs free energies (ΔG) of the protonated *Z* isomers of them are lower than their corresponding *E* isomers, while those of (*S*)-NAB is just the reverse. The chair conformation is still the most stable conformation for both *E* and *Z* isomers of (*S*)-NAB-H^+, but the pyridyl group is in equatorial position comparing the structure of non-protonated (*S*)-NAB.

The relative Gibbs free energies (ΔG_{298K}) for the *Z*-*E* interconversion of protonated TSNAs are from 93.79 to 111.68 kJ/mol, which are all larger than 80 kJ/mol (see Table 8). This fact indicates that protonation slightly influences the *Z*-*E* interconversion of TSNAs and due to the high activation energies, the interconversion of *E* and *Z* isomers of TSNAs and their pronated forms may not happen at room temperature. Thus, only in certain temperature range the peak-splitting phenomenon can be observed for the N-NO single bonds can rotate to form favored isomers for TSNAs and TSNAS-H^+ at higher temperature.

Additionally, protonation affects the dipole moment of molecules significantly. The dipole moments of the protonated TSNAs are in the range of 8.0-11.6 Debye, much larger than those of the non-protonated TSNAs (1.9-4.8 Debye). The difference of the calculated dipole moment between the *E* and *Z* isomers for TSNAs-H^+ is in the range of 0.7-2.1 Debye, whereas it is 0.1-0.5 Debye for free TSNAs. Furthermore, the computed dipole moments of the protonated *E* isomers are much larger than their corresponding *Z* forms. But for free TSNAs, no such trends are observed.

In previous experimental reports,[9] at pH 3.5 and 4.0, NNN was divided up into two peaks and NAT was eluted as one singled, while at pH 4.8, NNN elutes as one single peak and NAT was split up into two narrow peaks. The amount of protonated TSNAs in mobile phase at pH 3.5 are more than those at pH 4.8 for the more acidic solution. According to our calculations, the difference of dipole moments of protonated *E*/*Z* isomers and free *E*/*Z* isomers of NNN are 1.7 and 0.1 Debye, while those of NAT are 0.7 and 0.2 Debye, respectively, which totally agree with the experiment that the separation of *E*/*Z* isomers of NNN is easier than those of NAT in acidic solutions.

In summary, the *E*/*Z* isomers of TSNAs should be separated at room temperature theoretically, but the separation of them may be difficult because of the small dipole moment difference between the two non-protonated isomers, whereas it should be easier for protonated *E* and *Z* isomers because of the larger difference of their dipole moments. These should be the reasons why the split-up of the signal for NNN, NAT, NNK and NNAL into two peaks are very sensitive to the pH and temperature of the mobile-phase.

Table 7. Calculated proton affinity (PA) values of *E* and *Z* isomers of (*S*)-NNN (**1**) at M05/6-311++G(d,p) level

Species	PA (kJ/mol)
1-*Z*-conformer a	945.13665173
1-*Z*-conformer b	855.35417379
1-*Z*-conformer c	883.90962486
1-*E*-conformer a	936.33702326
1-*E*-conformer b	888.99502209
1-*E*-conformer c	844.32443053

Table 8. Calculated relative electronic energies (ΔE), Gibbs free energy (ΔG_{298K}), enthalpy (ΔH_{298K}), equilibrium constants (K_{eq}), Boltzmann populations (*P*) and dipole moment (μ) for the isomerization of *Z* to *E* forms of TSNAs-H^+ at M05/6-311++G(d,p) level

Species	ΔE (kJ/mol)	ΔG_{298K} (kJ/mol)	ΔH_{298K} (kJ/mol)	K_{eq}	*P* (%)	μ (debye)
1-H^+-*Z*	0.00	0.00	0.00	18.76	95	7.79
1-H^+-*E*	9.65	7.26	9.35		5	9.51
1-H^+-TS	111.06	105.81	104.84		-	8.26
2-H^+-*Z*	0.00	0.00	0.00	3.81	79	10.63
2-H^+-*E*	3.94	3.31	4.09		21	11.38
2-H^+-TS	118.13	111.68	111.71		-	9.80
3-H^+-*Z*	0.00	0.00	0.00	0.81	45	7.92
3-H^+-*E*	2.33	-0.50	1.86		55	10.08
3-H^+-TS	99.53	93.79	93.80		-	9.28

Summary

The results of a detailed study of the *E*/*Z* isomers and their internal rotation TS in four TSNAs, using DFT methods with 6-311++G(2d,2p) and 6-311++G(d,p) basis sets, were presented. Mostly, the *E* isomers are more stable than *Z* isomers, while the *Z* isomers would be more stable when in protonation. Due to the higher barrier energies for interconversion of the isomers in the TSNAs and their protonated forms (> 80 kJ/mol), the calculated results predict the possibility of separation of their *E* and *Z* isomer forms. The NBO analysis and the values of the dipole moments were also reported for these compounds. The results explained mainly the origin of the peak-spliting signals of TSNAs in HPLC with lower pH and at room temperature are in relation to the higher rotation energies and the various dipole moments in various conditions.

Supplementary Data. Supplementary data are available with this paper through the journal Web site.

Acknowledgments. The authors would like to thank Professor Hua-Jie Zhu for his valuables suggestions. We are also grateful to the National Nature Science Foundation of

China (grant No. 21002099) and China Tobacco Yunnan Industrial Co., Ltd. (grant No. 2010JC11 and 2011JC08) for financial support. The support of the Supercomputing Center, CNIC, CAS for computer time is acknowledged too.

References

1. Shah, K. A.; Karnes, H. T. *Crit. Rev. Toxicol.* **2010**, *40*, 305.
2. Shah, K. A.; Peoples, M. C.; Halquist, M. S.; Rutan, S. C.; Karnes, H. T. *J. Pharmaceut. Biomed*. **2011**, *54*, 368.
3. Yang, Y.; Nie, H.; Li, C.; Bai, Y.; Li, N.; Liao, J.; Liu, H. *Talanta* **2010**, *82*, 1797.
4. Kavvadias, D.; Scherer, G.; Urban, M.; Cheung, F.; Errington, G.; Shepperd, J.; McEwan, M. *J. Chromatogr. B* **2009**, *877*, 1185.
5. Carmella, S. G.; Ye, M.; Upadhyaya, P.; Hecht, S. S. *Cancer Res*. **1999**, *59*, 3602.
6. Clayton, P. M.; Cunningham, A.; van Heemst, J. D. H. *Anal. Methods* **2010**, *2*, 1085.
7. Sleiman, M.; Maddalena, R. L.; Gundel, L. A.; Destaillats, H. *J. Chromatogr. A* **2009**, *1216*, 7899.
8. Li, C.; Chen, Z.; Wen, D.; Zhang, J.; Cong, W.; Yu, B.; Liao, Y.; Liu, H. *Electrophoresis* **2006**, *27*, 2152.
9. Jansson, C.; Paccou, A.; Osterdahl, B. G. *J. Chromatogr. A* **2003**, *1008*, 135.
10. Trushin, N.; Leder, G.; El-Bayoumy, K.; Hoffmann, D.; Beger, H.; Henne-Bruns, D.; Ramadani, M.; Prokopczyk, B. *Langenbecks Arch. Surg*. **2008**, *393*, 571.
11. Breyer-Pfaff, U.; Martin, H.-J.; Ernst, M.; Maser, E. *Drug Metab. Dispos*. **2004**, *32*, 915.
12. McCorquodale, E. M.; Boutrid, H.; Colyer, C. L. *Anal. Chim. Acta* **2003**, *496*, 177.
13. Hecht, S. S.; Spratt, T. E.; Trushin, N. *Carcinogenesis* **1997**, *18*, 1851.
14. Wu, W.; Ashley, D. L.; Watson, C. H. *Anal. Chem*. **2003**, *75*, 4827.
15. Roohi, H.; Deyhimi, F.; Ebrahimi, A. *J. Mol. Struct. (Theochem)* **2001**, *543*, 299.
16. Roohi, H.; Deyhimi, F.; Ebrahimi, A.; Khanmohammady, A. *J. Mol. Struct. (Theochem)* **2005**, *718*, 123.
17. Chow, Y. L.; Colón, C. J. *Can. J. Chem*. **1968**, *46*, 2827.
18. do Monte, S. A.; Ventura, E.; da Costa, T. F.; Santana, S. R. D. *Struct. Chem*. **2011**, *22*, 497.
19. Novak, I.; Kovac, B. *Chem. Phys. Lett*. **2007**, *445*, 129.
20. Miura, M.; Sakamoto, S.; Yamaguchi, K.; Ohwada, T. *Tetrahedron Lett*. **2000**, *41*, 3637.
21. Carmella, S. G.; McIntee, E. J.; Chen, M.; Hecht, S. S. *Carcinogenesis* **2000**, *21*, 839.
22. *Gaussian 03*, Revision E.01, Frisch, M. J.; Trucks, G. W.; Schlegel, H. B.; Scuseria, G. E.; Robb, M. A.; Cheeseman, J. R.; Montgomery, J. A., Jr.; Vreven, T.; Kudin, K. N.; Burant, J. C.; Millam, J. M.; Iyengar, S. S.; Tomasi, J.; Barone, V.; Mennucci, B.; Cossi, M.; Scalmani, G.; Rega, N.; Petersson, G. A.; Nakatsuji, H.; Hada, M.; Ehara, M.; Toyota, K.; Fukuda, R.; Hasegawa, J.; Ishida, M.; Nakajima, T.; Honda, Y.; Kitao, O.; Nakai, H.; Klene, M.; Li, X.; Knox, J. E.; Hratchian, H. P.; Cross, J. B.; Bakken, V.; Adamo, C.; Jaramillo, J.; Gomperts, R.; Stratmann, R. E.; Yazyev, O.; Austin, A. J.; Cammi, R.; Pomelli, C.; Ochterski, J. W.; Ayala, P. Y.; Morokuma, K.; Voth, G. A.; Salvador, P.; Dannenberg, J. J.; Zakrzewski, V. G.; Dapprich, S.; Daniels, A. D.; Strain, M. C.; Farkas, O.; Malick, D. K.; Rabuck, A. D.; Raghavachari, K.; Foresman, J. B.; Ortiz, J. V.; Cui, Q.; Baboul, A. G.; Clifford, S.; Cioslowski, J.; Stefanov, B. B.; Liu, G.; Liashenko, A.; Piskorz, P.; Komaromi, I.; Martin, R. L.; Fox, D. J.; Keith, T.; Al-Laham, M. A.; Peng, C. Y.; Nanayakkara, A.; Challacombe, M.; Gill, P. M. W.; Johnson, B.; Chen, W.; Wong, M. W.; Gonzalez, C.; Pople, J. A. Gaussian, Inc.: Wallingford CT, 2004.
23. Tong, X. G.; Wu, G. S.; Huang, C. G.; Lu, Q.; Wang, Y. H.; Long, C. L.; Luo, H. R.; Zhu, H. J.; Cheng, Y. X. *J. Nat. Prod*. **2010**, *73*, 1160.
24. Li, L. C.; Ren, J.; Liao, T. G.; Jiang, J. X.; Zhu, H. *J. Eur. J. Org. Chem*. **2007**, 1026.
25. Zhao, Y.; Schultz, N. E.; Truhlar, D. G. *J. Chem. Phys*. **2005**, *123*, 161103.
26. Reed, A. E.; Curtiss, L. A.; Weinhold, F. *Chem. Rev.* **1988**, *88*, 899.
27. Martin, F.; Zipse, H. *J. Comput. Chem*. **2005**, *26*, 97.
28. Hwang, S.; Jiang, Y. H.; Chung D. S. *Bull. Korean Chem. Soc.* **2005**, *26*, 585.
29. Krebs, B.; Mandt, J. *Chem. Ber.* **1975**, *108*, 1130.
30. Ohwada, T.; Miura, M.; Tanaka, H.; Sakamoto, S.; Yamaguchi, K.; Ikeda, H.; Inagaki, S. *J. Am. Chem. Soc.* **2001**, *123*, 10164.